Eclética Química Journal

Original article

iq.unesp.br/ecletica

| Vol. 47 | n. 1 | 2022 |

Photoperoxidation of ciprofloxacin antibiotic in aqueous medium using $Fe_{3-x}O_{4-y}$-TiO_2 particles as catalyst

Ismael Laurindo Costa Junior[1+], Kevin Augusto Ferreira[1], Cesar Augusto Kappes[1], Renata Mello Giona[1]

1. Federal Technological University of Paraná, Chemistry Department, Medianeira, Brazil.

+Corresponding author: Ismael Laurindo Costa Junior, **Phone:** +55 45999355163, **Email address:** isma_jr@hotmail.com

ARTICLE INFO

Article history:
Received: February 04, 2021
Accepted: September 01, 2021
Published: January 01, 2022

Section Editor: Assis Vicente Benedetti

Keywords
1. photocatalyst
2. emerging pollutants
3. oxidative processes

ABSTRACT: Conventional treatment processes are not effective in removing micropollutants such as antibiotics and other drugs present in wastewater, and degradation methods based on advanced oxidative processes become attractive. Herein, it was synthesized $Fe_{3-x}O_{4-y}$-TiO_2 particles by coprecipitation method and they were heat-treated at 100, 400, and 800 °C. The obtained solids were characterized by X-ray diffraction and thermogravimetric analysis and analytical determinations were performed using ultraviolet-visible (UV-Vis) spectrophotometry. The particles were evaluated in photoperoxidation processes on the degradation of the ciprofloxacin antimicrobial in an aqueous solution. The studies took place at pH 9; with an H_2O_2 concentration of 31 mg L^{-1} and particle mass 0.22 g L^{-1} previously defined and, in these conditions, degradation percentages between 40 and 85% were observed, with the removal in the Photo/H_2O_2/$Fe_{3-x}O_{4-y}$-TiO_2 800 °C. The kinetic study performed for this process revealed the process adjusts to the first-order kinetics during the 120 min of reaction. The use of the catalyst can be attractive with the potential for degradation of the studied antimicrobial.

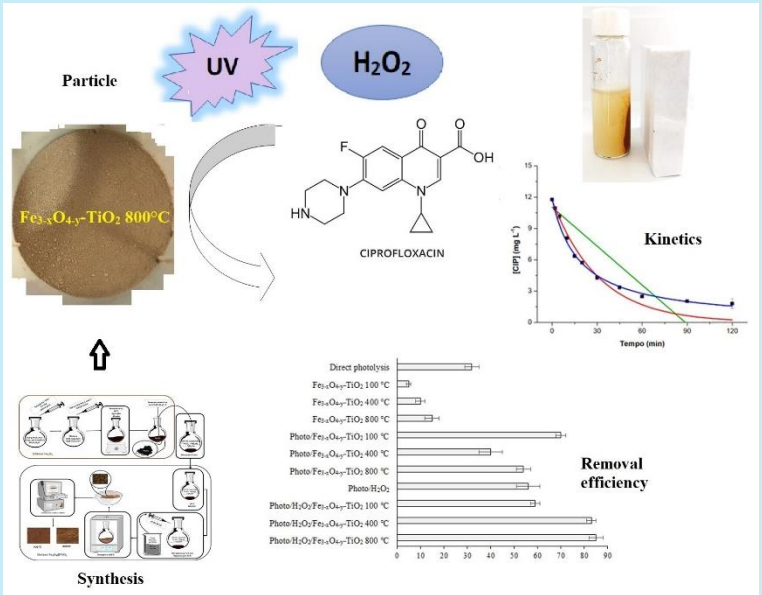

1. Introduction

Studies on residual drugs in the environment are topics of great relevance today (Costa Junior *et al.*, 2014). With the growth of the world population, the consumption of medicines has increased significantly in the last decades; as a result, these compounds are found in sewage treatment plant effluents, in water supplies, and various environmental compartments (Bound *et al.*, 2006; Luo *et al.*, 2014; Rogowska *et al.*, 2020).

One of the groups of residual drugs that attracts attention is antibiotics due to their potential effect on the development of resistant bacteria in the environment (Barancheshme and Munir, 2019; Karkman *et al.*, 2018). An example of an antimicrobial is ciprofloxacin (CIP), which belongs to the fluoroquinolone class and is widely used in human and veterinary medicine. Its excretion rate can reach 65% in urine and 25% in feces (Frade *et al.*, 2014; Halling-Sørensen *et al.*, 2000).

The discharge of domestic and industrial sewage in surface waters is one of the main routes of dispersion of emerging contaminants, especially drugs. Thus, the effective concentration of emerging pollutants, such as antibiotics, in the various environmental matrices directly depends on the efficiency of the treatment processes applied to wastewater in treatment plants (Leung *et al.*, 2012; Wu *et al.*, 2016).

The treatment methods used in sewage treatment plants are based mainly on conventional processes (physical and biochemical operations), aimed at stabilizing organic matter, removing nutrients, and disinfecting. Thus, effective degradation of these new contaminants is practically nonexistent (Oliveira *et al.*, 2020; Rajasulochana and Preethy, 2016). Some studies have suggested the removal of residual drugs in the treated sewage through the evaluation of input and output parameters in biological treatment systems (Sim *et al.*, 2010; Verlicchi *et al.*, 2012). However, other studies resulted only in the transfer of pollutants to sludge and sediments by sorption mechanisms, with no degradation or effective treatment (Barret *et al.*, 2010; Liu *et al.*, 2019; Piai *et al.*, 2020).

Considering the bioactive and persistent nature of organic micropollutants, the need for advanced treatments for their removal in wastewater is urgent. Some advanced oxidative processes (AOPs), such as ozonation, homogeneous and heterogeneous photocatalysis, are promising for pollutants degradation (Ciccotti *et al.*, 2015; Hörsing *et al.*, 2012; Hyland *et al.*, 2012; Souza *et al.*, 2018).

In heterogeneous photocatalysis, titanium dioxide (TiO_2) based catalysts have great viability and applicability to degrade a wide variety of pollutants. Its main advantages are its electronic properties, chemical stability, nontoxicity, and low cost (Rasalingam *et al.*, 2014; Yang *et al.*, 2005). Catalysts can be applied immobilized on supports or in suspension. When suspended, the separation step is a limitation of the process that involves time and costs. Magnetic particles have been extensively studied as a support for many hybrid materials, like TiO_2 (Borges *et al.*, 2015; Fabbri *et al.*, 2019; Pang *et al.*, 2012).

The association of TiO_2 photocatalytic and Fe_3O_4 magnetic properties has been explored in the proposition of core@shell particles (Ciccotti *et al.*, 2015; Noval *et al.*, 2019; Wei *et al.*, 2009). One of the advantages of using a magnetic material is that the catalyst could be easily removed from the reaction system through the application of an external magnetic field, also facilitating its recovery during the process steps (Dorigon *et al.*, 2017; Wu *et al.*, 2008).

In this work, heat-treated $Fe_{3-x}O_{4-y}$-TiO_2 magnetic particles were prepared and applied as catalysts in the degradation of the CIP antibiotic by heterogeneous photoperoxidation processes.

2. Materials and Methods

2.1 Reagents: standards and solutions

Ciprofloxacin (CIP) was purchased as an analytical standard for chromatography ($C_{17}H_{19}ClFN_3O_3$, Sigma-Aldrich) with 99.98% purity. Stock solutions of this drug were prepared at 1000 mg L^{-1}, swollen in ultrapure water and kept at 4 °C under refrigeration, protected from light. In the photocatalysis reactions, hydrogen peroxide (H_2O_2, Alphatec) was used.

Buffer solutions based on potassium phosphate (K_3PO_4, Exodus), anhydrous monobasic potassium phosphate (KH_2PO_4, Exodus), dibasic potassium phosphate (K_2HPO_4, Alphatec) and phosphoric acid were used for the reaction media 85% (H_3PO_4, Moderna). According to the pH ranges of the expeiments, adjustments were done using hydrochloric acid (HCl, Dinâmica) and sodium hydroxide (NaOH, Moderna) 0.01 mol L^{-1}. In the synthesis of particles, iron chloride III hexahydrate ($FeCl_3.6H_2O$, Dinâmica); iron chloride II ($FeCl_2$, Exodus), ammonium hydroxide (NH_4OH, Anhydrol); absolute ethyl alcohol (C_2H_6O, Dinâmica) and 97% IV titanium isopropoxide ($Ti[OCH(CH_3)_2]_4$, Sigma-Aldrich) were used.

Eclética Química Journal, vol. 47, n. 1, 2022, 55-63
ISSN: 1678-4618
DOI: 10.26850/1678-4618eqj.v47.1.2022.p55-63

2.2 Synthesis and characterization of $Fe_{3-x}O_{4-y}$-TiO_2 particles

The synthesis of Fe_3O_4 particles was performed using the modified coprecipitation method (Dorigon *et al.*, 2017; Wu *et al.*, 2008). Briefly, 10.8 g of $FeCl_3.6H_2O$ were added to a reaction flask containing 25 mL of 1.0 mol L^{-1} HCl aqueous solution and 50 mL of ultrapure water. In another flask, a solution of $FeCl_2$ was prepared to maintain the proportion of 2:1 in mol (Fe^{3+}/Fe^{2+}). This solution was transferred drop by drop, with the aid of a syringe, to the reaction flask containing the $FeCl_3.6H_2O$ in acidic solution, resulting in a ratio of 0.04 mol of Fe^{3+} to 0.02 mol of Fe^{2+}. Then, 250 mL of a 1.5 mol L^{-1} NaOH solution was added to the Fe^{3+}/Fe^{2+} mixture, followed by constant heating at 60 °C and stirring for 40 min under N_2 atmosphere. The black and magnetic solid obtained composed of Fe_3O_4 was thoroughly washed with ultrapure water until neutral pH, and then it was kept in suspension.

For the TiO_2 coating step, in a round-bottom flask with 250 mL capacity, 20 mL of the Fe_3O_4 suspension obtained in the previous step and 80 mL of absolute ethyl alcohol were added, followed by homogenization in an ultrasonic bath for 5 min. The pH suspension was adjusted to 9 by the addition of concentrated NH_4OH. In another flask, 24 mL of titanium isopropoxide IV 97% were added and diluted in 136 mL of ethyl alcohol, and 20 mL aliquots were added to the Fe_3O_4 suspension under homogenization for 15 min in an ultrasonic bath after each insertion.

The system remained at rest for 24 h and then it was dried in an oven at 100 °C. The solid was broken up into a mortar and divided into three parts, one set aside and the other two portions subjected to heat treatment at 400 and 800 °C, respectively, in a muffle furnace. After cooling, 1 mL of each solid was measured in a 5 mL beaker previously weighted on an analytical balance and the corresponding mass was obtained. Density was calculated by the ratio between mass and volume.

X-ray diffraction (XRD) patterns were measured using an empyrean diffractometer operating from 2 to 50° with a residence time of 2° min^{-1}.

Thermogravimetric analyzes (TGA) were performed on a Perkin Elmer STA 6000 TGA analyzer, with approximately 8 mg of the sample, which was placed on open platinum and preheated to 100 °C for 5 min. The measurements were carried out in a nitrogen atmosphere at a flow rate of 20 mL min^{-1} and a heating rate of 10 °C min^{-1}, using a heating range of up to 600 °C.

2.3 Analytical measures and photoperoxidation tests

For quantification of CIP, solutions with concentrations ranging from 1 to 25 mg L^{-1} at pH 9 were prepared for the calibration curve and were used to identify the maximum absorption band of CIP. The measurements were made by using a single beam scanning ultraviolet-visible (UV/VIS) molecular absorption spectrophotometer (PerkinElmer ™ LAMBDA XLS), in the range of 200 to 400 nm with a resolution of 2 nm. Quartz cuvettes with an optical path of 1 cm were used.

In the photoperoxidation tests, a reactor was used, consisting of a 57 × 47 × 47 cm^3 metal box equipped with four low-pressure mercury lamps (15 W) (OSRAM ™ Germicidal), used as a source of UV radiation and fixed at the top about 20 cm away from the solutions. The internal temperature remained around 45 °C after 20 min of stabilization. Inside, four 250 mL glass containers were placed on four magnetic stirrers (Fisatom). The initial CIP concentration was 10 mg L^{-1}, and aliquots of the solution were taken at regular intervals over the 120 min time.

A kinetic study was performed for the best treatment observed. The determination of the rate of degradation of target molecules and their respective concentrations (order of reaction) is an important step in the study of the kinetics of chemical reactions. The order of the reaction is understood as the dependence of the speed of the reaction with the concentration, where C_0 is the initial reagent concentration, and C is the reagent concentration after a reaction time (t) (Sarkar *et al.*, 2015).

If dC/dT satisfies Eq. 1, n is the order of the reaction.

$$\frac{dC}{dt} = -k.C^n \quad (1)$$

When n = 0 (zero order reaction), n = 1 (first order reaction) and n = 2 (second order reaction), Eq. 1 will lead to Eqs. 2–4, respectively.

$$C = C_0 - k_0 \cdot t \quad (2)$$

$$C = C_0 \cdot e^{-k1 \cdot t} \quad (3)$$

$$C = \frac{C_0}{1 + C_0 \cdot k_2 \cdot t} \quad (4)$$

In the photodegradation studies involving organic micropollutants, employed to assess persistence and susceptibility to ultraviolet radiation, the models

Eclética Química Journal, vol. 47, n. 1, 2022, 55-63
ISSN: 1678-4618
DOI: 10.26850/1678-4618eqj.v47.1.2022.p55-63

represented in Eqs. 2–4 are commonly applied for kinetic evaluation (Carlson *et al.*, 2015).

The experimental data obtained in the photoperoxidation tests catalyzed by the synthesized particles were evaluated in terms of the adjustments of the kinetic models (Eqs. 2–4) using the originPro 8.0 software. The decay of the CIP concentration was verified during the test and the half-life times were determined.

3. Results and discussion

3.1 Catalyst characterization

From the synthesis, it was obtained 7.9 g of $Fe_{3-x}O_{4-y}$-TiO_2 particles and they presented densities of 0.35 g mL^{-1} for the particles treated at 100 °C, 0.5 g mL^{-1} for 400 °C, and 0.6 g mL^{-1} for 800 °C (Fig. 1). This increase in density possibly resulted from the modification of the particle structure and the elimination of residual inputs from the synthesis. The magnetism of the particles was qualitatively evaluated in the presence of a neodymium magnet and, as shown in Fig. 1, $Fe_{3-x}O_{4-y}$-TiO_2 with heat treatments of 100 and 400 °C is magnetic, while the solid treated at 800 °C has lost its magnetic property upon heat treatment.

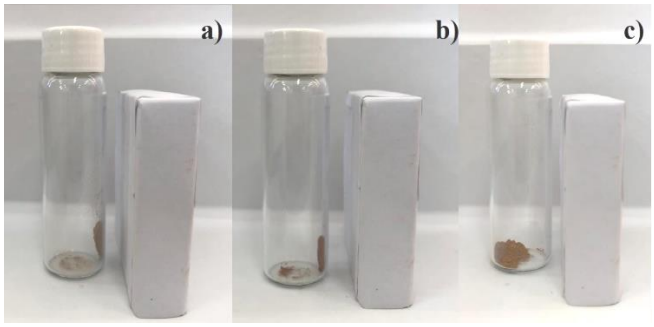

Figure 1. $Fe_{3-x}O_{4-y}$-TiO_2 being attract by a neodymium magnet. Treatments at **(a)** 100 °C **(b)** 400 °C and **(c)** 800 °C.

The crystallographic structures of the products were analyzed by powder XRD. The particles treated at 100 °C do not show peaks of a crystalline structure, suggesting an amorphous structure (Fig. 2a). Interestingly, the increase in temperature directly influenced the crystallinity of the system, with a predominance of α-Fe_2O_3 particles derived from the amorphous magnetite of the system, which is also reflected in the reduction of magnetism when heated to 800 °C (Fig. 1c).

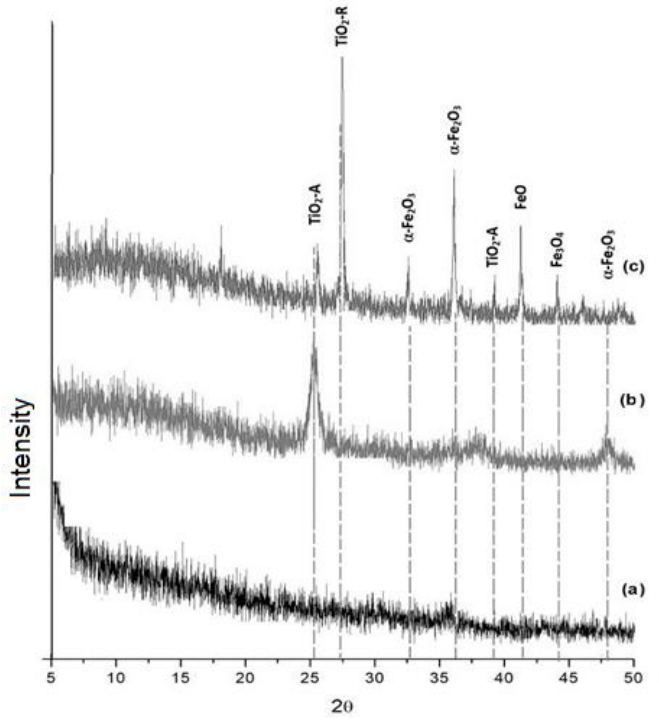

Figure 2. $Fe_{3-x}O_{4-y}$-TiO_2 XRD patterns in treatments at **(a)** 100 °C **(b)** 400 °C and **(c)** 800 °C.

In the particles treated at 400 °C (Fig. 2b), two main peaks were identified, the first referring to the TiO_2 anatase phase (25°) and the second to α-Fe_2O_3 phase (48°) (Khashan *et al.*, 2017). For the treatment at 800 °C, several peaks were observed, with the occurrence of TiO_2 anatase (25 and 39°), and rutile TiO_2 (27°), α-Fe_2O_3 (33 and 35°), FeO (42°) and Fe_3O_4 (44°) (Noval *et al.*, 2019).

The results of XRD indicate that the thermal treatments performed caused a structural modification in the synthesized particle, and the decrease in the magnetic property is due to the conversion of magnetite (Fe_3O_4) in oxides, such as α-Fe_2O_3 and FeO. Thus, it was assumed that the particles have a complex mixed composition of these compounds and, therefore, were denoted as $Fe_{3-x}O_{4-y}/TiO_2$. These hypotheses are reinforced by the TGA curves (Fig. 3).

From the TGA curves, it was determined a mass loss of approximately 25% of $Fe_{3-x}O_{4-y}$-TiO_2 particles synthesized at 100 °C. The first loss occurred between 50–150 °C and is related to the evaporation of alcohol and water residues adsorbed in the system. In the range of 150 to 350 °C, there is a loss that resulted from the decomposition of organic substances, and from 350 °C, total decomposition occurred, with crystallization beginning at high temperatures, generating a stable coating for the particles (Khashan *et al.*, 2017).

Eclética Química Journal, vol. 47, n. 1, 2022, 55-63
ISSN: 1678-4618
DOI: 10.26850/1678-4618eqj.v47.1.2022.p55-63

The particles treated at 400 and 800 °C did not show significant mass loss since they were previously subjected to a higher temperature. From TGA curves and XRD, it is possible to infer that the mass losses in the particles treated at 400 and 800 °C are lower than particles treated at 100 °C because the heating in the thermal treatment promoted structural changes. In addition, the TGA curves corroborate the predominance of the stable iron oxides identified in the XRD for the treatment of 800 °C.

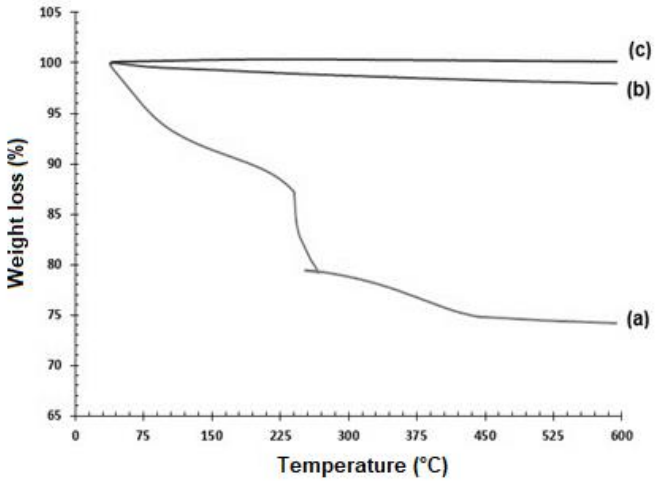

Figure 3. Thermogravimetric analyzes curves obtained for $Fe_{3-x}O_{4-y}$-TiO_2 synthesized in treatments **(a)** 100 °C **(b)** 400 °C and **(c)** 800 °C.

3.2 Application of synthesized particles in the photoperoxidation of ciprofloxacin

The absorption spectrum of the CIP drug with a concentration of 5 mg L^{-1} and pH 9 has a maximum absorption band at 278 nm, which is covered in the medium ultraviolet (Fig. 4).

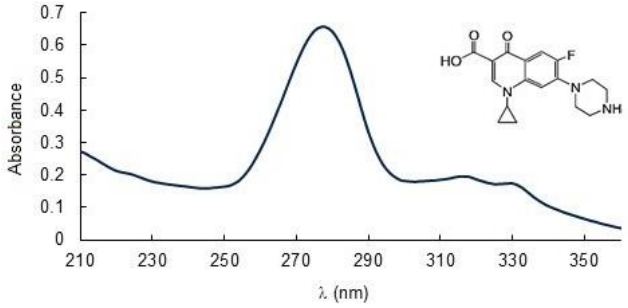

Figure 4. Ultraviolet-visible absorption spectrum in aqueous solution with a concentration of 5 mg L^{-1} of CIP and pH = 9.

Because of the molecular structure of CIP, its ionic forms depend on the pH. A cationic form is predominant in solution pH below 5.9 (up to pKa = 5.9), zwitterionic form is present in a neutral medium (5.9 < pKa < 8.9), and the anionic form is dominant at alkaline pH (pKa > 8.9) (Carabineiro *et al.*, 2012). Given that the photoperoxidation experiment was conducted at pH 9, the predominance of the anionic form of CIP is expected.

As for the surface of the photocatalyst, the pH_{PCZ} of the TiO_2 was 7.5 (Borges *et al.*, 2016). Under the conditions studied, the surface charge will also be negative, indicating that the possible removal of CIP by adsorption is unlikely, thus possibly not contributing to the results obtained through the photoperoxidation catalyzed by $Fe_{3-x}O_{4-y}$-TiO_2 particles. It is possible that, if adsorption phenomena still occur, the CIP molecules might be oxidized by reacting directly with the positive gap of the semiconductor valence layer, although this reaction is less likely (Mourão *et al.*, 2009; Nogueira and Jardim, 1998).

To evaluation the particles, the processes of direct photolysis, homogeneous photocatalysis (Photo/H_2O_2), and heterogeneous photocatalysis (Photo/$Fe_{3-x}O_{4-y}$-TiO_2 and Photo/H_2O_2/$Fe_{3-x}O_{4-y}$-TiO_2) were compared (Fig. 5). It was observed that the removal of the CIP antibiotic occurred in all tested processes.

No differences were observed between the process of direct photolysis and photocatalysis in the presence of particles without peroxidation. Thus, in these processes, the removals ranged from 36 to 56%. This behavior is possibly related to the mass of particles used (0.22 g L^{-1}) that may have impaired irradiation or also due to the need for more than 120 min for degradation.

The systems (Photo/H_2O_2/$Fe_{3-x}O_{4-y}$-TiO_2) with the heat treatments of 400 and 800 °C were the photocatalysts that presented the best performance, showing a percentage of degradation greater than 80%. This system was 30% more efficient than the direct photolysis process, indicating that the materials improved the photoperoxidation process (68%). Also, results showed that the particles with heat treatment of 100 °C presented low degradation efficiency, indicating that the absence of crystalline structures of the particles in the Photo/H_2O_2/$Fe_{3-x}O_{4-y}$-TiO_2 particle impairs the degradation of the CIP in the medium tested.

Eclética Química Journal, vol. 47, n. 1, 2022, 55-63
ISSN: 1678-4618
DOI: 10.26850/1678-4618eqj.v47.1.2022.p55-63

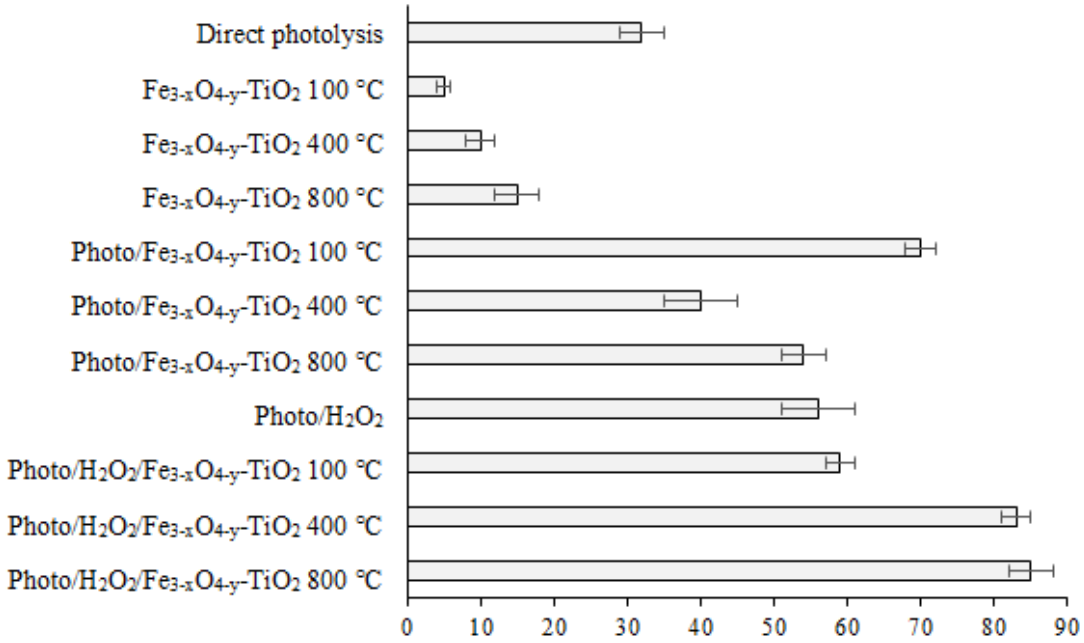

Figure 5. Ciprofloxacin removal during the tested degradation processes. Experimental condition: t = 120 min, $[CIP]_0$ = 10 mg L^{-1}, pH = 9, H_2O_2 = 31 mg L^{-1} and [Particles] = 0.22 g L^{-1}.

Hence, direct photolysis alone could not be used as an important procedure for the removal of CIP from aqueous solutions. As can be seen in Fig. 5, the removal of CIP via adsorption onto $Fe_{3-x}O_{4-y}$-TiO_2 (6 to 14 %) was lower in comparison to the photocatalysis process.

Fe_3O_4@SiO_2@TiO_2 particles with heat treatment of 500 and 600 °C were evaluated as a heterogeneous photocatalysis with H_2O_2 in a reactor composed of six lamps of 8 W, pH of 5.5, and CIP degradations of 83 and 95%, respectively, were reported over a test time of 90 min (Teixeira *et al.*, 2017). These results were similar to those obtained in this study.

Considering the photocatalyzed peroxidation process by the particles synthesized in the 800 °C heat treatment exhibited the best performance (Fig. 4), this system was evaluated through the kinetic study (Fig. 6).

It was observed that the most intense degradation of the CIP occurs in the first 60 min; this time interval corresponds to the dynamic range and might be related to factors such as the maximum amount of H_2O_2 favorable to the mechanism or the competition with by-products that were formed (Fioreze *et al.*, 2014). After 60 min, low degradation rates were observed, indicating that the system tends to stabilize, keeping the concentration of residual CIP constant.

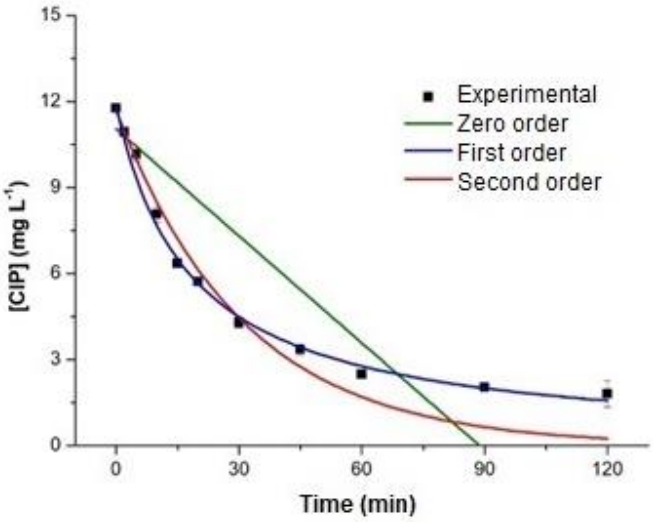

Figure 6. Kinetic study of the photo/H_2O_2/$Fe_{3-x}O_{4-y}$-TiO_2 process applied to CIP degradation. T = 120 min, $[CIP]_0$ = 12 mg L^{-1}, pH = 9, H_2O_2 = 31 mg L^{-1} and [Particles] = 0.22 g L^{-1}.

From the R^2 coefficients (Tab. 1), it was possible to determine that the model that presented the best fitting of experimental data was the first order with R^2 of 99.7%; such a model assumes that, in a speed reaction, it is directly dependent on the concentration of the reagents.

Eclética Química Journal, vol. 47, n. 1, 2022, 55-63
ISSN: 1678-4618
DOI: 10.26850/1678-4618eqj.v47.1.2022.p55-63

Table 1. Kinetic data for Photo/H_2O_2/$Fe_{3-x}O_{4-y}$-TiO_2 process. t = 120 min, $[CIP]_0$ = 12 mg L^{-1}, pH = 9, H_2O_2 = 31 mg L^{-1} and [Particles] = 0.22 g L^{-1}.

Zero order			First order			Second order		
k_0 (mg L^{-1} min^{-1})	$t_{1/2}$ (min)	R^2	k_1 (min^{-1})	$t_{1/2}$ (min)	R^2	k_2 (L mg^{-1} min^{-1})	$t_{1/2}$ (min)	R^2
0.12 (± 0.02)	44.5	80.9	0.05 (± 0.002)	16.9	99.7	0.03 (± 0.003)	23.1	97.9

Based on the first-order model, it was observed that, in 16.9 min, the CIP concentration was reduced to half of its initial value. The rate constant (k) was 0.05 min^{-1}. Similarly, a study using Fe_3O_4@SiO_2@TiO_2 in CIP photodegradation presented the first-order constant of 0.017 min^{-1} (Teixeira *et al.*, 2017). Also, the degradation of CIP with an initial concentration of 20 mg L^{-1} was studied by the photocatalysis process using a Fe_3O_4@TiO_2@C-dot particle exposed to a mercury vapor lamp. The kinetic model followed first-order with a k = 0.0154 min^{-1} during 150 min of testing (Das *et al.*, 2016).

A heterogeneous photocatalysis study using TiO_2 obtained 57% efficiency in CIP removal over 120 min of testing in a reactor equipped with 16 W UV lamps. The reported model was also first-order with a rate constant of 0.0063 min^{-1} (Hassani *et al.*, 2015).

Comparing the data obtained here for the photodegradation of CIP with studies reported in the literature, it is clear that $Fe_{3-x}O_{4-y}$-TiO_2 heat-treated at 800 °C is a promising catalyst for CIP degradation.

4. Conclusions

Here, the facile and reproducible preparation of $Fe_{3-x}O_{4-y}$-TiO_2 particles was reported, combining the use of the TiO_2 catalyst with the magnetic properties of iron oxide.

In the conditions explored, the photocatalysts showed degradation percentages between 40 and 85%, in which the Photo/H_2O_2/$Fe_{3-x}O_{4-y}$-TiO_2 process with the particles synthesized in the 800 °C heat treatment exhibited the best performance.

The kinetic study revealed that $Fe_{3-x}O_{4-y}$-TiO_2 catalyst followed first-order kinetics during the 120 min reaction. The use of a large amount of catalyst has some limitations, such as low degradation, for example, possibly because the dispersed particles interfere with the incident radiation. Despite this, the process is attractive, since it eliminates the need for a robust wastewater post-treatment step to remove the suspended catalyst.

Thus, although other factors must be evaluated for real scale usage, such as the analysis and removal of by-products formed, using, for example, chromatography liquid techniques coupled to mass spectrometry, the heterogeneous photocatalysis process using the synthesized particles is a promising treatment in the CIP degradation.

Authors' contribution

Conceptualization: Costa Junior, I. L.; Giona, R. M.; Ferreira, K. A.; Kappes, C. A.
Data curation: Costa Junior, I. L.; Giona, R. M.
Formal Analysis: Costa Junior, I. L.; Ferreira, K. A.; Kappes, C. A.
Funding acquisition: Not applicable
Investigation: Costa Junior, I. L.; Giona, R. M.; Ferreira, K. A.; Kappes, C. A.
Methodology: Costa Junior, I. L.; Giona, R. M.
Project administration: Costa Junior, I. L.
Resources: Not applicable
Software: Not applicable
Supervision: Costa Junior, I. L.
Validation: Costa Junior, I. L.; Ferreira, K. A.; Kappes, C. A.
Visualization: Giona, R. M.
Writing – original draft: Costa Junior, I. L.; Giona, R. M.; Ferreira, K. A.; Kappes, C. A.
Writing – review & editing: Costa Junior, I. L.; Giona, R. M.

Data availability statement

All data sets were generated or analyzed in the current study.

Funding

Not applicable.

Acknowledgments

We are grateful to the Federal Technological University of Paraná for their assistance in the course of this study.

References

Barancheshme, F.; Munir, M. Development of antibiotic resistance in wastewater treatment plants. In *Antimicrobial resistance: A global threat*; IntechOpen, 2019; pp 75–91. https://doi.org/10.5772/intechopen.81538

Barret, M.; Carrère, H.; Latrille, E.; Wisniewski, C.; Patureau, D. Micropollutant and sludge characterization for modeling sorption equilibria. *Environ. Sci. Technol.* **2010**, *44* (3), 1100–1106. https://doi.org/10.1021/es902575d

Borges, E.; García, D. M.; Hernández, T.; Ruiz-Morales, J. C.; Esparza, P. Supported photocatalyst for removal of emerging contaminants from wastewater in a continuous packed-bed photoreactor configuration. *Catalysts* **2015**, *5* (1), 77–87. https://doi.org/10.3390/catal5010077

Borges, S. S.; Xavier, L. P. S.; Silva, A. C.; Aquino, S. F. Imobilização de dióxido de titânio em diferentes materiais suporte para o emprego em fotocatálise heterogênea. *Quím. Nova* **2016**, 39 (7), 836–844. https://doi.org/10.5935/0100-4042.20160106

Bound, J. P.; Kitsou, K.; Voulvoulis, N. Household disposal of pharmaceuticals and perception of risk to the environment. *Environ. Toxicol. Pharmacol.* **2006**, *21* (3), 301–307. https://doi.org/10.1016/j.etap.2005.09.006

Carabineiro, S. A. C.; Thavorn-amornsri, T.; Pereira, M. F. R.; Serp, P.; Figueiredo, J. L. Comparison between activated carbon; carbon xerogel and carbon nanotubes for the adsorption of the antibiotic ciprofloxacin. *Catal. Today* **2012**, (1), 29–34. https://doi.org/10.1016/j.cattod.2011.08.020

Carlson, J. C.; Stefan, M. I.; Parnis, J. M.; Metcalfe, C. D. Direct UV photolysis of selected pharmaceuticals, personal care products and endocrine disruptors in aqueous solution. *Water Res.* **2015**, *84*, 350–361. https://doi.org/10.1016/j.watres.2015.04.013

Ciccotti, L.; Vale, L. A. S.; Hewer, T. L. R.; Freire, R. S. Fe_3O_4@TiO_2 preparation and catalytic activity in heterogeneous photocatalytic and ozonation processes. *Catal. Sci. Technol.* **2015**, *5* (2), 1143–1152. https://doi.org/10.1039/C4CY01242A

Costa Junior, I. L.; Pletsch, A. L.; Torres, Y. R. Ocorrência de fármacos antidepressivos no meio ambiente: Revisão. *Rev. Virtual Quím.* **2014**, *6* (5), 1408–1431. https://doi.org/10.5935/1984-6835.20140092

Das, R. K.; Kar, J. P.; Mohapatra S. Enhanced photodegradation of organic pollutants by carbon quantum dot (CQD) deposited Fe_3O_4@mTiO_2 nano-pom-pom balls. *Ind. Eng. Chem. Res.* **2016**, *55* (20), 5902–5910. https://doi.org/10.1021/acs.iecr.6b00792

Dorigon, L.; Frota, J. P. R. A.; Kreutz, J. C.; Giona R. M.; Moisés, M. P.; Bail, A. Synthesis and characterization of mesoporous silica-coated magnetite containing cetyltrimethylammonium bromide and evaluation on the adsorption of sodium dodecylbenzenesulfonate. *Appl. Surf. Sci.* **2017**, *420*, 954–962. https://doi.org/10.1016/j.apsusc.2017.05.249

Fabbri, D.; López-Muñoz, M. J.; Daniele, A.; Medana, C.; Calza, P. Photocatalytic abatement of emerging pollutants in pure water and wastewater effluent by TiO_2 and Ce-ZnO: Degradation kinetics and assessment of transformation products. *Photochem. Photobiol. Sci.* **2019**, *18* (4), 845–852. https://doi.org/10.1039/C8PP00311D

Fioreze, M.; Santos, E. P.; Schmachtenberg, N. Processos oxidativos avançados: Fundamentos e aplicação ambiental. *Revista Eletrônica em Gestão; Educação e Tecnologia Ambiental* **2014**, *18* (1), 79–91. https://doi.org/10.5902/2236117010662

Frade, V. M. F; Dias, M.; Teixeira, A. C. S. C.; Palma, M. S. A. Environmental contamination by fluoroquinolones. *Braz. J. Pharm. Sci.* **2014**, *50* (1), 41–54. https://doi.org/10.1590/S1984-82502011000100004

Halling-Sørensen, B.; Holten Lützhøft, H.-C.; Andersen, H. R.; Ingerslev, F. Environmental risk assessment of antibiotics: Comparison of mecillinam; trimethoprim and ciprofloxacin. *J. Antimicrob. Chemother.* **2000**, *46* (Sippl.1), 53–58. https://doi.org/10.1093/jac/46.suppl_1.53

Hassani, A.; Khataee, A.; Karaca, S. Photocatalytic degradation of ciprofloxacin by synthesized TiO_2 nanoparticles on montmorillonite: Effect of operation parameters and artificial neural network modeling. *J. Mol. Catal. A Chem.* **2015**, *409*, 149–161. https://doi.org/10.1016/j.molcata.2015.08.020

Hörsing, M.; Kosjek, T.; Andersen, H. R.; Heath, E.; Ledin, A. Fate of citalopram during water treatment with O_3, ClO_2, UV and fenton oxidation. *Chemosphere* **2012**, *89* (2), 129–135. https://doi.org/10.1016/j.chemosphere.2012.05.024

Hyland, K. C.; Dickenson, E. R. V.; Drewes, J. E.; Higgins, C. P. Sorption of ionized and neutral emerging trace organic compounds onto activated sludge from different wastewater treatment configurations. *Water Res.* **2012**, *46* (6), 1958–1968. https://doi.org/10.1016/j.watres.2012.01.012

Karkman, A.; Do, T. T.; Walsh, F.; Virta, M. P. J. Antibiotic-resistance genes in waste water. *Trends Microbiol.* **2018**, *26* (3), 220–228. https://doi.org/10.1016/j.tim.2017.09.005

Khashan, S; Dagher S; Tit N; Alazzam A; Obaidat I. Novel method for synthesis of Fe_3O_4@TiO_2 core/shell nanoparticles. *Surf. Coat. Technol.* **2017**, *322*, 92–98. https://doi.org/10.1016/j.surfcoat.2017.05.045

Leung, H. W.; Minh, T. B.; Murphy, M. B.; Lam, J. C. W.; So, M. K.; Martin, M.; Lam, P. K. S.; Richardson, B. J. Distribution; fate and risk assessment of antibiotics in sewage treatment plants in Hong Kong, South China. *Environ. Int.* **2012**, *42*, 1–9. https://doi.org/10.1016/j.envint.2011.03.004

Liu, F.; Nielsen, A. H.; Vollertsen, J. Sorption and degradation potential of pharmaceuticals in sediments from a stormwater retention pond. *Water* **2019**, **11** (3), 526. https://doi.org/10.3390/w11030526

Luo, Y.; Guo, W.; Ngo, H. H.; Nghiem, L. D.; Hai, F. I.; Zhang, J.; Liang, S.; Wang, X. C. A review on the occurrence of micropollutants in the aquatic environment and their fate and removal during wastewater treatment. *Sci. Total Environ.* **2014**, *473–474*, 619–641. https://doi.org/10.1016/j.scitotenv.2013.12.065

Mourão, H. A. J. L.; Mendonça, V. R; Malagutti, A. R.; Ribeiro, C. Nanoestruturas em fotocatálise: Uma revisão sobre estratégias de síntese de fotocatalisadores em escala nanométrica. *Quím. Nova* **2009**, *32* (8), 2181–2190. https://doi.org/10.1590/S0100-40422009000800032

Nogueira, R. F. P.; Jardim, W. F. A fotocatálise heterogênea e sua aplicação ambiental. *Quím. Nova* **1998**, *21* (1), 69–72. https://doi.org/10.1590/S0100-40421998000100011

Noval, V. E.; Carriazo, J. G. Fe_3O_4-TiO_2 and Fe_3O_4-SiO_2 core-shell powders synthesized from industrially processed magnetite (Fe_3O_4) microparticles. *Mat. Res.* **2019**, *22* (3), e20180660. https://doi.org/10.1590/1980-5373-mr-2018-0660

Oliveira, M.; Frihling, B. E. F.; Velasques, J.; Magalhães Filho, F. J. C.; Cavalheri, P. S; Migliolo, L. Pharmaceuticals residues and xenobiotics contaminants: Occurrence; analytical techniques and sustainable alternatives for wastewater treatment. *Sci. Total Environ.* **2020**, *705*, 135568. https://doi.org/10.1016/j.scitotenv.2019.135568

Pang, S. C.; Kho, S. Y.; Chin, S. F. Fabrication of magnetite/silica/titania core-shell nanoparticles. *J. Nanomater.* **2012**, *2012*, 427310. https://doi.org/10.1155/2012/427310

Piai, L; Blokland, M; van der Wal, A.; Langenhoff, A. Biodegradation and adsorption of micropollutants by biological activated carbon from a drinking water production plant. *J. Hazard. Mater.* **2020**, *388*, 122028. https://doi.org/10.1016/j.jhazmat.2020.122028

Rajasulochana, P.; Preethy, V. Comparison on efficiency of various techniques in treatment of waste and sewage water: A comprehensive review. *Resource-Efficient Technologies* **2016**, *2* (4), 175–184. https://doi.org/10.1016/j.reffit.2016.09.004

Rasalingam, S.; Peng, R.; Koodali, R. T. Removal of hazardous pollutants from wastewaters: Applications of TiO_2-SiO_2 mixed oxide materials. *J. Nanomater.* **2014**, *2014*, 617405. https://doi.org/10.1155/2014/617405

Rogowska, J.; Cieszynska-Semenowicz, M.; Ratajczyk, W.; Wolska, L. Micropollutants in treated wastewater. *Ambio* **2020**, *49*, 487–503. https://doi.org/10.1007/s13280-019-01219-5

Sarkar, S.; Chakraborty, S.; Bhattacharjee, C. Photocatalytic degradation of pharmaceutical wastes by alginate supported TiO_2 nanoparticles in packed bed photo reactor (PBPR). *Ecotoxicol. Environ. Saf.* **2015**, *121*, 263–270. https://doi.org/10.1016/j.ecoenv.2015.02.035

Sim, W.-J.; Lee, J.-W.; Oh, J.-E. Occurrence and fate of pharmaceuticals in wastewater treatment plants and rivers in Korea. *Environ. Pollut.* **2010**, *158* (5), 1938–1947. https://doi.org/10.1016/j.envpol.2009.10.036

Souza, F. S.; Silva, V. V.; Rosin, C. K.; Hainzenreder, L.; Arenzon, A.; Féris, L. A. Comparison of different advanced oxidation processes for the removal of amoxicillin in aqueous solution. *Environ. Technol.* **2018**, *39* (5), 549–557. https://doi.org/10.1080/09593330.2017.1306116

Teixeira, S.; Mora, H.; Blasse, L.-M.; Martins, P. M.; Carabineiro, S. A. C; Lanceros-Méndez, S.; Kühn, K.; Cuniberti, G. Photocatalytic degradation of recalcitrant micropollutants by reusable Fe_3O_4/SiO_2/TiO_2 particles. *J. Photochem. Photobiol. A Chem.* **2017**, *345*, 27–35. https://doi.org/10.1016/j.jphotochem.2017.05.024

Verlicchi, P.; Al Aukidy, M.; Zambello, E. Occurrence of pharmaceutical compounds in urban wastewater: Removal, mass load and environmental risk after a secondary treatment—A review. *Sci. Total Environ.* **2012**, *429*, 123–155. https://doi.org/10.1016/j.scitotenv.2012.04.028

Wei, J. H.; Leng, C. J.; Zhang, X. Z.; Li, W. H.; Liu, Z. Y.; Shi, J. Synthesis and magnetorheological effect of Fe_3O_4-TiO_2 nanocomposite. *J. Phys.: Conf. Ser.* **2009**, *149*, 012083. https://doi.org/10.1088/1742-6596/149/1/012083

Wu, W.; He, Q.; Jiang, C. Magnetic iron oxide nanoparticles: Synthesis and surface functionalization strategies. *Nanoscale Res. Lett.* **2008**, *3*, 397. https://doi.org/10.1007/s11671-008-9174-9

Wu, M.-H.; Que, C.-J.; Xu, G.; Sun, Y.-F.; Ma, J.; Xu, H.; Sun, R.; Tang, L. Occurrence; fate and interrelation of selected antibiotics in sewage treatment plants and their receiving surface water. *Ecotoxicol. Environ. Saf.* **2016**, *132*, 132–139. https://doi.org/10.1016/j.ecoenv.2016.06.006

Yang, J.; Chen, C.; Ji, H.; Ma, W.; Zhao, J. Mechanism of TiO_2-assisted photocatalytic degradation of dyes under visible irradiation: Photoelectrocatalytic study by TiO_2-film electrodes. *J. Phys. Chem. B* **2005**, *109* (46), 21900–21907. https://doi.org/10.1021/jp0540914

Eclética Química Journal, vol. 47, n. 1, 2022, 55-63
ISSN: 1678-4618
DOI: 10.26850/1678-4618eqj.v47.1.2022.p55-63